

# TorchXRyVision: A library of chest X-ray datasets and models

Joseph Paul Cohen<sup>S,M,Q,A</sup> Joseph D. Viviano<sup>Q</sup> Paul Bertin<sup>M,Q</sup> Paul Morrison<sup>Q,F</sup>  
 Parsa Torabian<sup>W</sup> Matteo Guarrera<sup>B,E,P</sup> Matthew P Lungren<sup>S,A</sup>  
 Akshay Chaudhari<sup>S,A</sup> Rupert Brooks<sup>N</sup> Mohammad Hashir<sup>M,Q</sup> Hadrien Bertrand<sup>Q</sup>  
<sup>S</sup>Stanford University <sup>M</sup>Université de Montréal <sup>Q</sup>Mila, Quebec AI Institute <sup>A</sup>Center for Artificial Intelligence in Medicine & Imaging (AIMI) <sup>N</sup>Nuance Communications <sup>F</sup>Fontbonne University <sup>W</sup>University of Waterloo <sup>B</sup>University of California, Berkeley <sup>P</sup>Politecnico di Torino <sup>E</sup>EURECOM  
 Correspondance: <https://github.com/mlmed/torchxrayvision/issues>

## Abstract

TorchXRyVision is an open source software library for working with chest X-ray datasets and deep learning models. It provides a common interface and common pre-processing chain for a wide set of publicly available chest X-ray datasets. In addition, a number of classification and representation learning models with different architectures, trained on different data combinations, are available through the library to serve as baselines or feature extractors.

**Keywords:** Chest X-ray, CXR, pre-trained models, datasets, representation learning, generalization, feature extraction, PyTorch

## 1. Introduction

Chest X-rays are the most common medical imaging test in the world and represent the bulk of medical computer vision publications and open medical imaging data in the deep learning community [UK NHS, 2019]. Yet despite the large number of datasets and publications, it can be difficult for researchers to properly compare previous work and to investigate generalization across different datasets. Even when data and code are available, small but important differences in dataset organization, processing, or training procedures can significantly impact the results. This makes establishing meaningful baselines a strenuous task for researchers. In addition, constantly re-implementing the same dataloaders is not the best use of time. There is a need for common software infrastructure.

TorchXRyVision<sup>1</sup> (XRV) was created to address this difficulty by establishing a reusable framework for reproducible research and consistent baseline experiments. A key design objective is to provide a clear interface and separation between datasets and models. The library provides a common interface to multiple available chest X-ray datasets, which can easily be swapped out during model training and evaluation. Common pre- and post-processing components are provided and the datasets are compatible with torchvision [Paszke et al., 2019] components for augmentation. We include pre-trained and easily downloadable models which can be used directly for baseline comparisons or to generate feature vectors for downstream tasks.

Three specific use cases where the project has already proved useful include:

---

1. <https://github.com/mlmed/torchxrayvision>

- **Evaluating models:** It is important to rigorously evaluate the robustness of models using multiple external datasets. However, associated clinical data with each dataset can vary greatly which makes it difficult to apply methods to multiple datasets. TorchXRyVision provides access to many datasets in a uniform way so that they can be swapped out with a single line of code. These datasets can also be merged and filtered to construct specific distributional shifts for studying generalization.
- **Developing models:** Making it easier for Deep Learning researchers to work on medical tasks. Pre-trained models are useful for baseline comparisons as well as feature extractors. These pre-trained models have already been used for transfer learning to related chest X-ray tasks such as patient severity scoring [Cohen et al., 2020a; Gomes et al., 2020a] and predicting aspects about a patients clinical trajectory [Cohen et al., 2020c; Gomes et al., 2020b; Maurya, 2020]. As illustrated in [Cherti and Jitsev, 2021] TorchXRyVision pre-trained models are used to study few-shot transfer learning. The pre-trained models are used as feature extractors of images for multi-modal models [Delbrouck et al., 2021; Soenksen et al., 2022]. In [Sundaram and Hulkund, 2021] the library is used for baseline models as well as to explore methods of generative adversarial network-based (GAN) data augmentation. The pre-trained models and training pipeline were used in [Tetteh et al., 2021] to study balancing batches while training on multiple datasets.
- **Studying model failures and limitations:** The many pre-trained models provided are not perfect and can be studied to determine how they fail, which can inform the development of better models. Also, the many datasets available in TorchXRyVision make it possible to study out-of-distribution generalization when covariate and concept shifts are present. The library was initially developed for this purpose in [Cohen et al., 2020b]. This library has already been used in work by [Robinson et al., 2021] which focused on studying shortcut learning caused by covariate shift in chest X-ray models. Work by [Viviano et al., 2020] explored failures in saliency maps using this library and special utilities are included to produce datasets with different types of covariate shift and spurious correlations. Work by [Cohen et al., 2021a] generated counterfactual explanations for model predictions using the classifiers and autoencoder in the library.

A key design consideration when developing this library was to follow an object-oriented approach. This turns the various components of an experiment into objects which can be easily swapped. The primary objects are datasets and models (including pre-trained weights). A suite of utilities for working with these objects are also included. The library is available in Python via pip with the package name `torchxrayvision` and is typically imported as `import torchxrayvision as xrv`. It is based on PyTorch [Paszke et al., 2019] and modeled after the torchvision library (hence the name). TorchXRyVision’s compatibility and conformity to established convention makes adoption intuitive for practitioners.

## 2. Models

The library is composed of core and baseline classifiers. Core classifiers are trained specifically for this library (initially trained for [Cohen et al., 2020b]) and baseline classifiers come from other papers that have been adapted to provide the same interface and work with

the same input pixel scaling as our core models (see `BENCHMARKS.md` on GitHub for current model performances). All models automatically resize input images (higher or lower using bilinear interpolation) to match the specified size they were trained on. This allows them to be easily swapped out for experiments. See §3.1 for details on image pro-processing. Pre-trained models are hosted on GitHub and automatically downloaded to the user’s local `~/torchxrayvision` directory.

## 2.1. Core Classifiers

Core pre-trained classifiers are provided as PyTorch Modules which are fully differentiable in order to work seamlessly with other PyTorch code. Models are specified using the “weights” parameter which have the general form of:

$$\underbrace{\text{densenet121}}_{\text{Architecture}} - \overbrace{\text{res224}}^{\text{Resolution}} - \underbrace{\text{rsna}}_{\text{Training dataset}}$$

Each pre-trained model aims to have 18 independent output classes as defined in `xrv.datasets.default_pathologies`. However, since not all datasets provide each pathology class, some will return NaN as the prediction of that pathology. The models indicating “all” as the dataset have been trained on as many datasets were available at the time. More details about each set of weights is available at the head of the `models.py` file. The current core classifiers were trained with data augmentation to improve generalization. According to best data augmentation parameters found in Cohen et al. [2019], each image was randomly rotated up to 45 degrees, translated up to 15% and scaled larger or smaller up to 10%. These models are trained using binary cross entropy losses, Adam optimizer [Kingma and Ba, 2014], a batch size of 64, and a learning rate of 0.001.

```
# DenseNet 224x224 model trained on multiple datasets
model = xrv.models.DenseNet(weights="densenet121-res224-all")
# DenseNet trained on just the RSNA Pneumonia dataset
model = xrv.models.DenseNet(weights="densenet121-res224-rsna")
# ResNet 512x512 model trained on multiple datasets
model = xrv.models.ResNet(weights="resnet50-res512-all")
```

## 2.2. Baseline Classifiers

Currently there are two baseline classifiers from other research groups which were added to make it easier to compare against TorchXRayVision core models. The models adhere to the same interface as the core models and can be easily swapped out. The first is a JFHealthcare model [Ye et al., 2020] trained on CheXpert data [Irvin et al., 2019] and the second is an official CheXpert model [Irvin et al., 2019] trained by the CheXpert team.

```
# DenseNet121 from JF Healthcare for the CheXpert competition
model = xrv.baseline_models.jfhealthcare.DenseNet()
# Official Stanford CheXpert model
model = xrv.baseline_models.chexpert.DenseNet()
```

The weights for the CheXpert model are very (6GB) and have been hosted on Academic Torrents [Cohen and Lo, 2014] as well as the Internet Archive.

### 2.3. Classifier Interface

Each classifier provides a field `model.pathologies` which aligns to the list of predictions that the model makes. Depending on the weights loaded this list will change. The predictions can be aligned to pathology names as follows:

```
predictions = model(img)[0] # 0 is first element of batch
dict(zip(model.pathologies,predictions.detach().numpy()))
# output:
{'Atelectasis': 0.3566849,
 'Consolidation': 0.72457345,
 'Infiltration': 0.8974177, ...}
```

Getting a specific output can be achieved as follows. The outputs remain part of the computation graph and can therefore be embedded in a larger network.

```
prediction = model(img)[: ,model.pathologies.index("Consolidation")]
```

### 2.4. Feature Extraction

The pre-trained models can also be used as features extractors for semi-supervised training or transfer learning tasks. A feature vector can be obtained for each image using the `model.features` function. The resulting size will vary depending on the architecture and the input image size. For some models there is a `model.features2` method that will extract features at a different point of the computation graph. Example UMAP visualizations [McInnes et al., 2018] of the features from different models is shown in Figure 1.

```
feats = model.features(img)
```

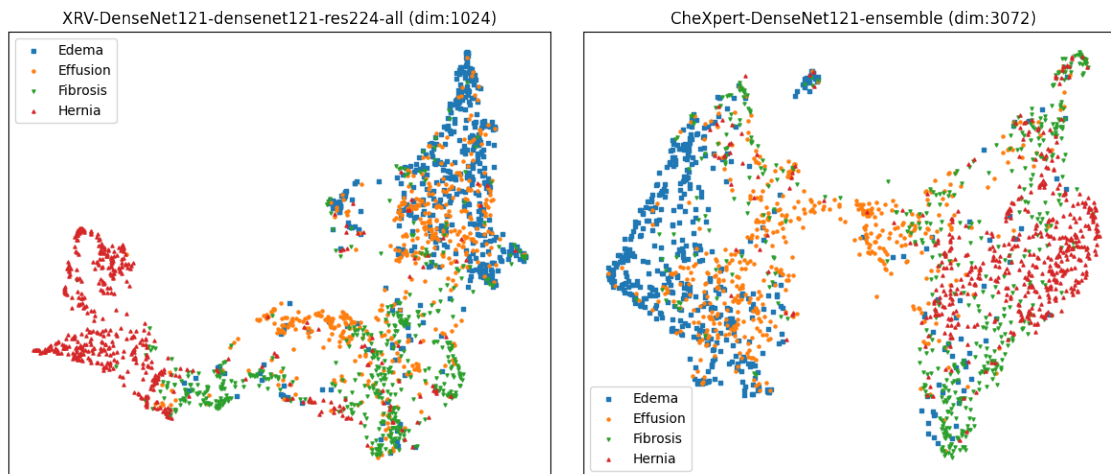


Figure 1: UMAP visualizations of the representations from different models. 2048 images, each containing only one of the 4 pathologies listed, are included in the UMAP.

## 2.5. Autoencoders

The library also provides a pre-trained autoencoder that is trained on the PadChest, NIH, CheXpert, and MIMIC datasets. This model was developed in [Cohen et al., 2021a] and provides a fixed latent representation. The goal of this model is to provide another representation extraction model which is not trained using supervised labels and has a decoder to reconstruct images from the latent representation.

```
ae = xrv.autoencoders.ResNetAE(weights="101-elastic")
z = ae.encode(image)
image2 = ae.decode(z)
%\end{code}
```

## 3. Datasets

The datasets in this library aim to fit a simple interface where the `imgpath` and `csvpath` are specified. Some datasets require more than one metadata file and for some the metadata files are packaged in the library so only the `imgpath` needs to be specified.

Documentation for each dataset class provides citation information and download links. When possible, metadata is included with the library so only the `imgpath` needs to be specified. When possible based on the license, datasets have been uploaded to Academic Torrents [Cohen and Lo, 2014]. Otherwise, the dataset can be downloaded from its origin by following the links provided in the class documentation.

```
dataset = xrv.datasets.VinBrain_Dataset(imgpath="./train",
                                       csvpath="./train.csv")
```

Each dataset object also supports the standard `transform` argument which takes PyTorch transforms. While standard transforms will be applied there may be issues in how they deal with the specific tensor shapes returned by the dataloader (`[1, RES, RES]` where `RES` is the image resolution)

```
transform = torchvision.transforms.Compose([xrv.datasets.XRayCenterCrop(),
                                           xrv.datasets.XRayResizer(224)])
```

Tables 1 and 2 display the total count of images and labels available per dataset.

### 3.1. Image pre-processing

Both models and datasets expect the image pixel values to be between `[-1024, 1024]`. The origin of this is arbitrary. The preprocessing of images used scales from the possible range of the images and not the min and max of the pixels. For example, if the image is 16-bit encoded then the possible pixels values are between 0 and 65,536 so this range will be mapped; not the min and max pixels of the specific image. The idea here is that we don't want to arbitrarily increase the contrast of an image because that could be removing information.

Table 1: Details of datasets that are included in this library. Number of images shows total images / usable frontal images. Useable frontal means images that are readable, have all necessary metadata, and are in AP, PA, AP Supine, or AP Erect view.

Name	# Images (Total/Frontal)		Citation	Geographic Region
National Library of Medicine Tuberculosis	800	/ 800	Jaeger et al. [2014]	USA+China
OpenI (National Library of Medicine)	7,470	/ 4,014	Demner-Fushman et al. [2016]	USA
ChestX-ray8 (NIH)	112,120	/ 112,120	Wang et al. [2017]	Northeast USA
RSNA Pneumonia Challenge	26,684	/ 26,684	Shih et al. [2019]	Northeast USA
CheXpert (Stanford University)	223,414	/ 191,010	Irvin et al. [2019]	Western USA
Google Labelling of NIH data	4,376	/ 4,376	Majkowska et al. [2019]	Northeast USA
MIMIC-CXR (MIT)	377,095	/ 243,324	Johnson et al. [2019]	Northeast USA
PadChest (University of Alicante)	158,626	/ 108,722	Bustos et al. [2020]	Spain
SIIM-ACR Pneumothorax Challenge	12,954	/ 12,954	Filice et al. [2020]	Northeast USA
COVID-19 Image Data Collection (CIDC)	866	/ 698	Cohen et al. [2020c]	Earth
StonyBrook COVID-19 RALO Severity	2,373	/ 2,373	Cohen et al. [2021b]	Northeast USA
Object-CXR (JF Healthcare)	9,000	/ 9,000	-	China
VinBrain VinDr-CXR	15,000	/ 15,000	Nguyen et al. [2020]	Vietnam

### 3.2. Dataset common fields

Each dataset contains a number of common fields. These fields are maintained when `xrv.datasets.SubsetDataset` and `xrv.datasets.MergeDataset` are used.

- `dataset.pathologies` a list of strings identifying the pathologies contained in this dataset. This list corresponds to the columns of the `.labels` matrix. Although it is called pathologies, the contents do not have to be pathologies and may simply be attributes of the patient.
- `dataset.labels` field is a NumPy matrix [Harris et al., 2020] which contains a 1, 0, or NaN for each pathology. Each column is a pathology and each row corresponds to an item in the dataset. A 1 represents that the pathology is present, 0 represents the pathology is absent, and NaN represents no information.
- `dataset.csv` field which holds a Pandas DataFrame [McKinney, 2010] of the metadata `.csv` file that is included with the data. For some datasets multiple metadata files have been merged together. It is largely a "catch-all" for associated data and the referenced publication should explain each field. Each row aligns with the elements of the dataset so indexing using `.iloc` will work. Alignment between the DataFrame and the dataset items will be maintained when using tools from this library.

If possible, each dataset's `.csv` will have some common fields of the `csv`. These will be aligned when datasets are merged together.

- `dataset.csv.patientid` is a unique id that will uniquely identify patients in the dataset. This is useful when trying to prevent patient overlap between train and test sets or in conjunction with the next field to observe patients over time.
- `dataset.csv.offset_day_int` is an integer time offset for the image in the unit of days. This is expected to be for relative times and has no guarantee to be an absolute time although for some datasets it is and is formatted in unix epoch time.

- `dataset.csv.view` is a string indicating the projection/view in which the chest X-ray was acquired. Most will be “PA”, “AP”, or “AP Supine”. A good discussion of views is contained in [Bustos et al., 2020].

### 3.3. Dataset tools

**Relabelling datasets** Working with dataset objects is a task that the library is designed to help with. Tasks such as aligning, composing, or taking a subset of a dataset are made easy using the functions discussed below. The function `xrv.datasets.relabel_dataset` will add, remove, and reorder the `.labels` field to have the same order as the `pathologies` argument passed to it. If a pathology is specified but doesn’t exist in the dataset then a NaN will be put in place of the label.

```
# Note: dataset is directly changed, no return value
xrv.datasets.relabel_dataset(xrv.datasets.default_pathologies, dataset)
```

**Filtering based on views** Specific views can be specified in the constructor to select only those views. This is only supported on datasets which have view information. Common views have been standardized to “PA”, “AP”, or “AP Supine”, but other non-standardized ones may exist. It is best to first load the dataset without filtering based on view and call `dataset.csv.view.unique()` to see what is available.

```
dataset = xrv.datasets.PC_Dataset(..., views=["PA", "AP", "AP Supine"])
```

**Ensuring one image per patient** The `unique_patients` argument will tell the dataset to only allow 1 image per patient. This only works on datasets which provide a `patientid`.

```
dataset = xrv.datasets.PC_Dataset(..., unique_patients=True)
```

**Obtaining summary statistics on a dataset** Simply printing the object will return counts for the available labels and their classes. This is also returned as a dictionary with the function `dataset.totals()`.

```
print(d_chex)
# Output:
CheX_Dataset num_samples=191010 views=['PA', 'AP']
{'Atelectasis': {0.0: 17621, 1.0: 29718},
 'Cardiomegaly': {0.0: 22645, 1.0: 23384},
 'Consolidation': {0.0: 30463, 1.0: 12982}, ...}
```

**Merging datasets together** The class `xrv.datasets.MergeDataset` can be used to merge multiple datasets together into a single dataset. This class takes in a list of dataset objects and assembles the datasets in order. This class will correctly maintain the `.labels`, `.csv`, and `.pathologies` fields and offer pretty printing.

```
dmerge = xrv.datasets.MergeDataset([dataset1, dataset2, ...])
# Output:
MergeDataset num_samples=261583
├─0 PC_Dataset num_samples=94825 views=['PA', 'AP']
├─1 RSNA_Pneumonia_Dataset num_samples=26684 views=['PA', 'AP']
├─2 NIH_Dataset num_samples=112120 views=['PA', 'AP']
├─3 SIIM_Pneumothorax_Dataset num_samples=12954
└─4 VinBrain_Dataset num_samples=15000 views=['PA', 'AP']
```

**Taking a subset of a dataset** When you only want a subset of a dataset the `SubsetDataset` class can be used. A list of indexes can be passed in and only those indexes will be present in the new dataset. This class will correctly maintain the `.labels`, `.csv`, and `.pathologies` fields and offer pretty printing.

```
dsubset = xrv.datasets.SubsetDataset(dataset, [0,5,60])
# Output:
SubsetDataset num_samples=3
└ of PC_Dataset num_samples=94825 views=['PA', 'AP']
```

For example this class can be used to create a dataset of only female patients by selecting that column of the csv file and using `np.where` to convert this vector into a list of indexes.

```
idxs = np.where(dataset.csv.PatientSex_DICOM=="F")[0]
dsubset = xrv.datasets.SubsetDataset(dataset, idxs)
# Output:
SubsetDataset num_samples=48308
└ of PC_Dataset num_samples=94825 views=['PA', 'AP']
```

### 3.4. Pathology and semantic masks

Masks for pathologies or semantic regions are also included for some datasets. These are useful for segmentation or for validating that a model is attributing importance to the correct area (as explored in [Viviano et al., 2020] and [Cohen et al., 2021a]).

Masks are not returned by the datasets by default; the constructor for the dataset must specify `pathology_masks=True` and/or `semantic_masks=True` for them to be returned. These are treated differently because pathology masks are associated with the `dataset.pathologies` while semantic masks are unrelated (such as segmentations of the lungs). If no pathology masks exist the data will not have those arguments available and won't be constructed. If images do not have masks available then the key `"pathology_masks"` on the sample will be empty. Example usage:

```
dataset = xrv.datasets.RSNA_Pneumonia_Dataset(imgpath="stage_2_train_images_jpg",
                                             views=["PA", "AP"],
                                             pathology_masks=True)
```

Each sample will have a `pathology_masks` dictionary where the index of each pathology (in `dataset.pathologies`) will correspond to a mask of that pathology (if it exists). There may be more than one mask per sample, but only one per pathology. For simplicity, if there



are multiple masks for a single pathology they will be merged together using a logical or. The resulting mask will be values between 0 and 1 of type `float`. Data augmentations will be performed to these masks as well using the same seed to ensure an identical transformation is applied.

```
sample["pathology_masks"][dataset.pathologies.index("Lung Opacity")]
```

## 4. Acknowledgements

We thank the following organizations for supporting this project in various ways: CIFAR (Canadian Institute for Advanced Research), Mila (Quebec AI Institute), University of Montreal, Stanford University's Center for Artificial Intelligence in Medicine & Imaging, and Carestream Health. We thank AcademicTorrents.com for making data available for our research.

## References

- Aurelia Bustos, Antonio Pertusa, Jose-Maria Salinas, and Maria de la Iglesia-Vayá. PadChest: A large chest x-ray image dataset with multi-label annotated reports. *Medical Image Analysis*, 1 2020. doi: 10.1016/j.media.2020.101797. URL <http://arxiv.org/abs/1901.07441>.
- Mehdi Cherti and Jenia Jitsev. Effect of large-scale pre-training on full and few-shot transfer learning for natural and medical images. *arXiv:2106.00116*, 5 2021. URL <http://arxiv.org/abs/2106.00116>.
- Joseph Paul Cohen and Henry Z. Lo. Academic Torrents: A Community-Maintained Distributed Repository. In *Annual Conference of the Extreme Science and Engineering Discovery Environment*, 2014. ISBN 978-1-4503-2893-7. doi: 10.1145/2616498.2616528. URL <http://doi.acm.org/10.1145/2616498.2616528>.
- Joseph Paul Cohen, Paul Bertin, and Vincent Frappier. Chester: A Web Delivered Locally Computed Chest X-Ray Disease Prediction System. 2019. URL <http://arxiv.org/abs/1901.11210>.
- Joseph Paul Cohen, Lan Dao, Paul Morrison, Karsten Roth, Yoshua Bengio, Beiyi Shen, Almas Abbasi, Mahsa Hoshmand-Kochi, Marzyeh Ghassemi, Haifang Li, and Tim Q Duong. Predicting COVID-19 Pneumonia Severity on Chest X-ray with Deep Learning. *Cureus Medical Journal*, 5 2020a. doi: 10.7759/cureus.9448. URL <http://arxiv.org/abs/2005.11856>.
- Joseph Paul Cohen, Mohammad Hashir, Rupert Brooks, and Hadrien Bertrand. On the limits of cross-domain generalization in automated X-ray prediction. *Medical Imaging with Deep Learning*, 2020b. URL <https://arxiv.org/abs/2002.02497>.
- Joseph Paul Cohen, Paul Morrison, Lan Dao, Karsten Roth, Tim Q Duong, and Marzyeh Ghassemi. COVID-19 Image Data Collection: Prospective Predictions Are the Future.

- Journal of Machine Learning for Biomedical Imaging (MELBA)*, 2020c. URL <https://github.com/ieee8023/covid-chestxray-dataset>.
- Joseph Paul Cohen, Rupert Brooks, Sovann En, Evan Zucker, Anuj Pareek, Matthew P. Lungren, and Akshay Chaudhari. Gifsplanation via Latent Shift: A Simple Autoencoder Approach to Counterfactual Generation for Chest X-rays. *Medical Imaging with Deep Learning*, 2 2021a. URL <https://openreview.net/forum?id=rnunjvgxAMt>.
- Joseph Paul Cohen, Beiyi Shen, Almas Abbasi, Mahsa Hoshmand-Kochi, Samantha Glass, Haifang Li, Matthew P. Lungren, Akshay Chaudhari, and Tim Q Duong. Radiographic Assessment of Lung Opacity Score Dataset. *Zenodo*, 2021b. URL <https://doi.org/10.5281/zenodo.4633999>.
- Alex J DeGrave, Joseph D Janizek, and Su-In Lee. AI for radiographic COVID-19 detection selects shortcuts over signal. *medRxiv*, page 2020.09.13.20193565, 1 2020. doi: 10.1101/2020.09.13.20193565. URL <http://medrxiv.org/content/early/2020/09/14/2020.09.13.20193565.abstract>.
- Jean-Benoit Delbrouck, Cassie Zhang, and Daniel Rubin. QIAI at MEDIQA 2021: Multimodal Radiology Report Summarization. In *Workshop on Biomedical Language Processing*. Association for Computational Linguistics, 2021. doi: 10.18653/v1/2021.bionlp-1.33. URL <https://www.aclweb.org/anthology/2021.bionlp-1.33>.
- Dina Demner-Fushman, Marc D. Kohli, Marc B. Rosenman, Sonya E. Shooshan, Laritza Rodriguez, Sameer Antani, George R. Thoma, and Clement J. McDonald. Preparing a collection of radiology examinations for distribution and retrieval. *Journal of the American Medical Informatics Association*, 2016. doi: 10.1093/jamia/ocv080.
- Ross W. Filice, Anouk Stein, Carol C. Wu, Veronica A. Arteaga, Stephen Borstelmann, Ramya Gaddikeri, Maya Galperin-Aizenberg, Ritu R. Gill, Myrna C. Godoy, Stephen B. Hobbs, Jean Jeudy, Paras C. Lakhani, Archana Laroia, Sundeep M. Nayak, Maansi R. Parekh, Prasanth Prasanna, Palmi Shah, Dharshan Vummidi, Kavitha Yaddanapudi, and George Shih. Crowdsourcing pneumothorax annotations using machine learning annotations on the NIH chest X-ray dataset. *Journal of Digital Imaging*, 2020. doi: 10.1007/s10278-019-00299-9.
- Douglas P. S. Gomes, Michael J. Horry, Anwaar Ulhaq, Manoranjan Paul, Subrata Chakraborty, Manash Saha, Tanmoy Debnath, and D. M. Motiur Rahaman. MAVIDH Score: A COVID-19 Severity Scoring using Chest X-Ray Pathology Features. 11 2020a. URL <http://arxiv.org/abs/2011.14983>.
- Douglas P. S. Gomes, Anwaar Ulhaq, Manoranjan Paul, Michael J. Horry, Subrata Chakraborty, Manas Saha, Tanmoy Debnath, and D. M. Motiur Rahaman. Potential Features of ICU Admission in X-ray Images of COVID-19 Patients. 9 2020b. URL <http://arxiv.org/abs/2009.12597>.
- Charles R Harris, K Jarrod Millman, Stéfan J van der Walt, Ralf Gommers, Pauli Virtanen, David Cournapeau, Eric Wieser, Julian Taylor, Sebastian Berg, Nathaniel J Smith,

- Robert Kern, Matti Picus, Stephan Hoyer, Marten H van Kerkwijk, Matthew Brett, Allan Haldane, Jaime Fernández del Río, Mark Wiebe, Pearu Peterson, Pierre Gérard-Marchant, Kevin Sheppard, Tyler Reddy, Warren Weckesser, Hameer Abbasi, Christoph Gohlke, and Travis E Oliphant. Array programming with NumPy. *Nature*, 9 2020. doi: 10.1038/s41586-020-2649-2. URL <https://doi.org/10.1038/s41586-020-2649-2>.
- Jeremy Irvin, Pranav Rajpurkar, Michael Ko, Yifan Yu, Silvana Ciurea-Ilcus, Chris Chute, Henrik Marklund, Behzad Haghgoo, Robyn Ball, Katie Shpanskaya, Jayne Seekins, David A. Mong, Safwan S. Halabi, Jesse K. Sandberg, Ricky Jones, David B. Larson, Curtis P. Langlotz, Bhavik N. Patel, Matthew P. Lungren, and Andrew Y. Ng. CheXpert: A Large Chest Radiograph Dataset with Uncertainty Labels and Expert Comparison. In *AAAI Conference on Artificial Intelligence*, 2019. URL <http://arxiv.org/abs/1901.07031>.
- Stefan Jaeger, Sema Candemir, Sameer Antani, Yi-Xiang J. Wang, Pu-Xuan Lu, and George Thoma. Two public chest X-ray datasets for computer-aided screening of pulmonary diseases. *Quantitative imaging in medicine and surgery*, 4(6), 2014. ISSN 2223-4292. doi: 10.3978/J.ISSN.2223-4292.2014.11.20. URL <https://pubmed.ncbi.nlm.nih.gov/25525580/>.
- Alistair E. W. Johnson, Tom J. Pollard, Seth J. Berkowitz, Nathaniel R. Greenbaum, Matthew P. Lungren, Chih-ying Deng, Roger G. Mark, and Steven Horng. MIMIC-CXR: A large publicly available database of labeled chest radiographs. *Nature Scientific Data*, 2019. doi: 10.1038/s41597-019-0322-0. URL <http://arxiv.org/abs/1901.07042>.
- Diederik Kingma and Jimmy Ba. Adam: A Method for Stochastic Optimization. *International Conference on Learning Representations*, 2014. ISSN 09252312. doi: 10.1145/1830483.1830503. URL <http://arxiv.org/abs/1412.6980>.
- Anna Majkowska, Sid Mittal, David F. Steiner, Joshua J. Reicher, Scott Mayer McKinney, Gavin E. Duggan, Krish Eswaran, Po-Hsuan Cameron Chen, Yun Liu, Sreenivasa Raju Kalidindi, Alexander Ding, Greg S. Corrado, Daniel Tse, and Shravya Shetty. Chest Radiograph Interpretation with Deep Learning Models: Assessment with Radiologist-adjudicated Reference Standards and Population-adjusted Evaluation. *Radiology*, 2019. doi: 10.1148/radiol.2019191293. URL <http://pubs.rsna.org/doi/10.1148/radiol.2019191293>.
- Aniket Maurya. Predicting intubation support requirement of patients using Chest X-ray with Deep Representation Learning. 10 2020. doi: 10.13140/RG.2.2.18271.69282. URL <http://arxiv.org/abs/2011.01787><http://dx.doi.org/10.13140/RG.2.2.18271.69282>.
- Leland McInnes, John Healy, and James Melville. UMAP: Uniform Manifold Approximation and Projection for Dimension Reduction. 2 2018. URL <http://arxiv.org/abs/1802.03426>.
- Wes McKinney. Data Structures for Statistical Computing in Python. In *Python in Science Conference*, 2010. doi: 10.25080/Majora-92bf1922-00a.
- Jose G. Moreno-Torres, Troy Raeder, Rocío Alaiz-Rodríguez, Nitesh V. Chawla, and Francisco Herrera. A unifying view on dataset shift in classification. *Pattern Recognition*, 1 2012. ISSN 0031-3203. doi: 10.1016/J.PATCOG.2011.06.019.

- Ha Q. Nguyen, Khanh Lam, Linh T. Le, Hieu H. Pham, Dat Q. Tran, Dung B. Nguyen, Dung D. Le, Chi M. Pham, Hang T. T. Tong, Diep H. Dinh, Cuong D. Do, Luu T. Doan, Cuong N. Nguyen, Binh T. Nguyen, Que V. Nguyen, Au D. Hoang, Hien N. Phan, Anh T. Nguyen, Phuong H. Ho, Dat T. Ngo, Nghia T. Nguyen, Nhan T. Nguyen, Minh Dao, and Van Vu. VinDr-CXR: An open dataset of chest X-rays with radiologist’s annotations. 12 2020. URL <http://arxiv.org/abs/2012.15029>.
- Adam Paszke, Sam Gross, Francisco Massa, Adam Lerer, James Bradbury, Gregory Chanan, Trevor Killeen, Zeming Lin, Natalia Gimelshein, Luca Antiga, Alban Desmaison, Andreas Köpf, Edward Yang, Zach DeVito, Martin Raison, Alykhan Tejani, Sasank Chilamkurthy, Benoit Steiner, Lu Fang, Junjie Bai, and Soumith Chintala. PyTorch: An Imperative Style, High-Performance Deep Learning Library. *Neural Information Processing Systems*, 12 2019. URL <https://arxiv.org/abs/1912.01703>.
- David Powers. Evaluation: from precision, recall and F-measure to ROC, informedness, markedness and correlation. *Journal of Machine Learning Technologies*, 2011.
- Caleb Robinson, Anusua Trivedi, Marian Blazes, Anthony Ortiz, Jocelyn Desbiens, Sunil Gupta, Rahul Dodhia, Pavan K. Bhatraju, W. Conrad Liles, Aaron Lee, Jayashree Kalpathy-Cramer, and Juan M. Lavista Ferres. Deep learning models for COVID-19 chest x-ray classification: Preventing shortcut learning using feature disentanglement. *medRxiv*, 2021. doi: 10.1101/2021.02.11.20196766. URL <https://www.medrxiv.org/content/10.1101/2021.02.11.20196766v1>.
- George Shih, Carol C. Wu, Safwan S. Halabi, Marc D. Kohli, Luciano M. Prevedello, Tessa S. Cook, Arjun Sharma, Judith K. Amorosa, Veronica Arteaga, Maya Galperin-Aizenberg, Ritu R. Gill, Myrna C.B. Godoy, Stephen Hobbs, Jean Jeudy, Archana Laroia, Palmi N. Shah, Dharshan Vummidi, Kavitha Yaddanapudi, and Anouk Stein. Augmenting the National Institutes of Health Chest Radiograph Dataset with Expert Annotations of Possible Pneumonia. *Radiology: Artificial Intelligence*, 1(1):e180041, 1 2019. ISSN 2638-6100. doi: 10.1148/ryai.2019180041. URL <https://pubs.rsna.org/doi/abs/10.1148/ryai.2019180041>.
- Luis R. Soenksen, Yu Ma, Cynthia Zeng, Leonard D. J. Boussioux, Kimberly Villalobos Carballo, Liangyuan Na, Holly M. Wiberg, Michael L. Li, Ignacio Fuentes, and Dimitris Bertsimas. Integrated multimodal artificial intelligence framework for healthcare applications. 2 2022. doi: 10.48550/arxiv.2202.12998. URL <https://arxiv.org/abs/2202.12998>.
- Shobhita Sundaram and Neha Hulkund. GAN-based Data Augmentation for Chest X-ray Classification. In *KDD - Applied Data Science for Healthcare Workshop*, 7 2021. URL <https://arxiv.org/abs/2107.02970>.
- Enoch Tetteh, Joseph D. Viviano, David Kruege, Yoshua Bengio, and Joseph Paul Cohen. Multi-Domain Balanced Sampling Improves Out-of-Distribution Generalization of Chest X-ray Pathology Prediction Models. *Medical Imaging meets NeurIPS*, 2021.
- UK NHS. Diagnostic Imaging Dataset Annual Statistical Release 2018-19. Technical report, United Kingdom National Health Service, 2019. URL <https://www.england.nhs.uk/...>

[nhs.uk/statistics/statistical-work-areas/diagnostic-imaging-dataset/diagnostic-imaging-dataset-2018-19-data/](https://nhs.uk/statistics/statistical-work-areas/diagnostic-imaging-dataset/diagnostic-imaging-dataset-2018-19-data/).

Joseph D. Viviano, Becks Simpson, Francis Dutil, Yoshua Bengio, and Joseph Paul Cohen. Saliency is a Possible Red Herring When Diagnosing Poor Generalization. In *International Conference on Learning Representations (ICLR)*, 2020. URL <http://arxiv.org/abs/1910.00199>.

Xiaosong Wang, Yifan Peng, Le Lu, Zhiyong Lu, Mohammadhadi Bagheri, and Ronald M. Summers. ChestX-ray8: Hospital-scale Chest X-ray Database and Benchmarks on Weakly-Supervised Classification and Localization of Common Thorax Diseases. In *Computer Vision and Pattern Recognition*, 2017. doi: 10.1109/CVPR.2017.369. URL <http://arxiv.org/abs/1705.02315>.

Wenwu Ye, Jin Yao, Hui Xue, and Yi Li. Weakly Supervised Lesion Localization With Probabilistic-CAM Pooling, 2020. URL <https://arxiv.org/abs/2005.14480>.

Qingyu Zhao, Ehsan Adeli, Adolf Pfefferbaum, Edith V Sullivan, and Kilian M Pohl. Confounder-Aware Visualization of ConvNets. *arXiv:1907.12727*, 2019. URL <https://github.com/QingyuZhao/Confounder-Aware-CNN->.

## Appendix A. Extra Model Information

### A.1. Model Calibration

As described in [Cohen et al., 2019] and [Cohen et al., 2020b], Eq. 1 can be applied to calibrate the output of the model so that they can be compared with a piece-wise linear transformation. The goal is to make a prediction of 0.5 the estimated decision boundary based on held out test data. For each disease, we computed the optimal operating point of the ROC curve by maximizing the difference (*True positive rate - False positive rate*) on a hold out test set. It corresponds to the threshold which maximizes the informativeness of the classifier [Powers, 2011]. This is computed with the held out test subset of the dataset being used for training, as the model is intended to be evaluated on one of the other datasets. Also keep in mind that doesn't change the AUC on the test set, it is just for a nice calibrated probability output so you can use  $\text{pred} > 0.5$  to get a prediction.

$$f_{opt}(x) = \begin{cases} \frac{x}{2opt} & x \leq opt \\ 1 - \frac{1-x}{2(1-opt)} & otherwise \end{cases} \quad (1)$$

## Appendix B. Extra Dataset Information

Table 2: Labels available for each dataset, the total number of positive examples for each indication across all datasets, and the total number of example in each dataset, and the sum over each row in the right column. The COVID-19 datasets are excluded from this table because they have many unique pathologies.

	NIH	RSNA	NIH Google	PadChest	CheX	MIMIC	OpenI	NLMTB	SIIM	VinBrain	ObjectCXR	Total Positive Labels
Air Trapping				X								3438
Aortic Atheromatosis				X								1728
Aortic Elongation				X								8116
Aortic Enlargement										X		3067
Atelectasis	X			X	X	X	X			X		96,679
Bronchiectasis				X								1547
Calcification										X		452
Calcified Granuloma							X					193
Cardiomegaly	X			X	X	X	X			X		86,196
Consolidation				X	X	X				X		31,203
Costophrenic Angle Blunting				X								4244
Edema	X			X	X	X	X					82,689
Effusion	X			X	X	X	X			X		156,156
Emphysema	X			X			X					3708
Enlarged Cardiomeastinum					X	X						16,843
Fibrosis	X			X			X					2717
Flattened Diaphragm				X								535
Foreign Object											X	4500
Fracture			X	X	X	X	X					15,499
Granuloma				X			X					2999
Hemidiaphragm Elevation				X								1609
Hernia	X			X			X					1881
Hilar Enlargement				X								4867
ILD										X		386
Infiltration	X			X			X			X		34,296
Lung Lesion					X	X	X			X		13,676
Lung Opacity		X	X		X	X	X			X		158,919
Mass	X			X			X					6691
Nodule/Mass			X							X		1431
Nodule	X		X	X			X			X		10,334
Pleural Other					X	X						4586
Pleural Thickening	X			X			X			X		8764
Pneumonia	X	X		X	X	X	X					34,239
Pneumothorax	X		X	X	X	X	X		X	X		38,513
Pulmonary Fibrosis										X		1617
Scoliosis				X								5569
Tuberculosis				X				X				1165
Tube				X								6807
<b>Total Examples</b>	<b>112,120</b>	<b>26,684</b>	<b>4376</b>	<b>108,722</b>	<b>191,010</b>	<b>243,324</b>	<b>4014</b>	<b>800</b>	<b>12,954</b>	<b>15,000</b>	<b>9000</b>	<b>728,004</b>

Table 3: Counts of pathology and semantic masks available for each dataset.

Task	NIH	RSNA	SIIM-ACR	VinBrain	CIDC
Pneumothorax	(BBox) 98		(Seg) 3,576	(BBox) 96	
Lung Opacity		(Seg) 6,012		(BBox) 1,322	
Atelectasis	(BBox) 180			(BBox) 186	
Effusion	(BBox) 153			(BBox) 1,032	
Cardiomegaly	(BBox) 146			(BBox) 2,300	
Infiltration	(BBox) 123			(BBox) 613	
Pneumonia	(BBox) 120				
Mass	(BBox) 85				
Nodule	(BBox) 79				
Nodule/Mass				(BBox) 826	
Aortic enlargement				(BBox) 3,067	
Pleural_Thickening				(BBox) 1,981	
Calcification				(BBox) 452	
Interstitial lung disease				(BBox) 386	
Consolidation				(BBox) 353	
Lung					(Seg) 425

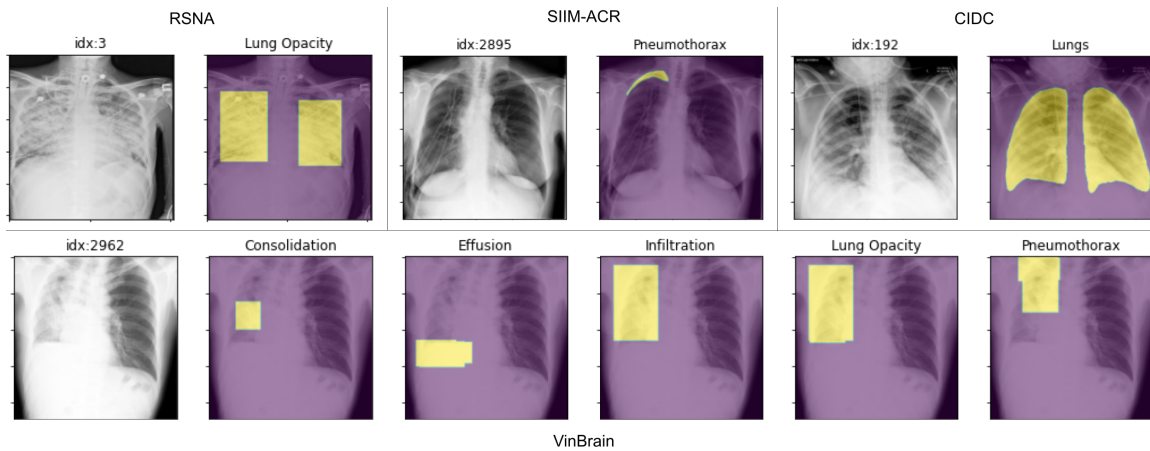


Figure 2: Example images and corresponding mask information available from multiple datasets. Some are bounding boxes and some are more exact segmentations.



## Appendix C. Distribution shift tools

A *covariate shift* between two data distributions arises when some extraneous variable confounds with the variables of interest in the first dataset differently than in the second [Moreno-Torres et al., 2012]. Covariate shifts between the training and test distribution in a machine learning setting can lead to models which generalize poorly, and this phenomenon is commonly observed in CXR models trained on a small dataset and deployed on another one [Zhao et al., 2019; DeGrave et al., 2020]. We provide tools to simulate covariate shifts in these datasets so researchers can evaluate the susceptibility of their models to these shifts, or explore mitigation strategies.

```
d = xrv.datasets.CovariateDataset(d1 = # dataset1 with a specific condition.  
                                d1_target = # target label to predict.  
                                d2 = # dataset2 with a specific condition.  
                                d2_target = #target label to predict.  
                                mode="train", # train, valid, or test.  
                                ratio=0.75)
```

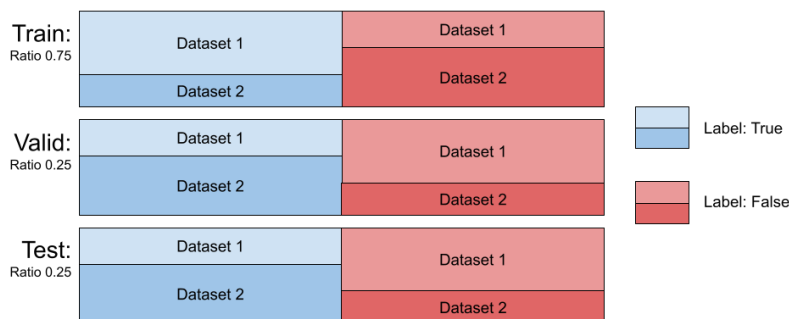


Figure 3: A CovariateDataset example of how the data would be split with a ratio of 0.75 specified. The target label will be balanced 50/50 in each split but the ratio of the origin dataset will be varied.

The class `xrv.datasets.CovariateDataset` takes two datasets and two arrays representing the labels. It returns samples for the output classes with a specified ratio of examples from each dataset, thereby introducing a correlation between any dataset-specific nuisance features and the output label. This simulates a covariate shift. The test split can be set up with a different ratio than the training split; this setup has been shown to both decrease generalization performance and exacerbate incorrect feature attribution [Viviano et al., 2020]. See Figure 4 for a visualization of the effect the ratio parameter has on the mean class difference when correlating the view (each dataset) with the target label. The effect seen with low ratios is due to the majority of the positive labels being drawn from the first dataset, where in the high ratios, the majority of the positive labels are drawn from the second dataset. With any ratio, the number of samples returned will be the same in order to provide

controlled experiments. The dataset has 3 modes, train sampled using the provided ratio and the valid and test dataset are sampled using  $1-\text{ratio}$ .

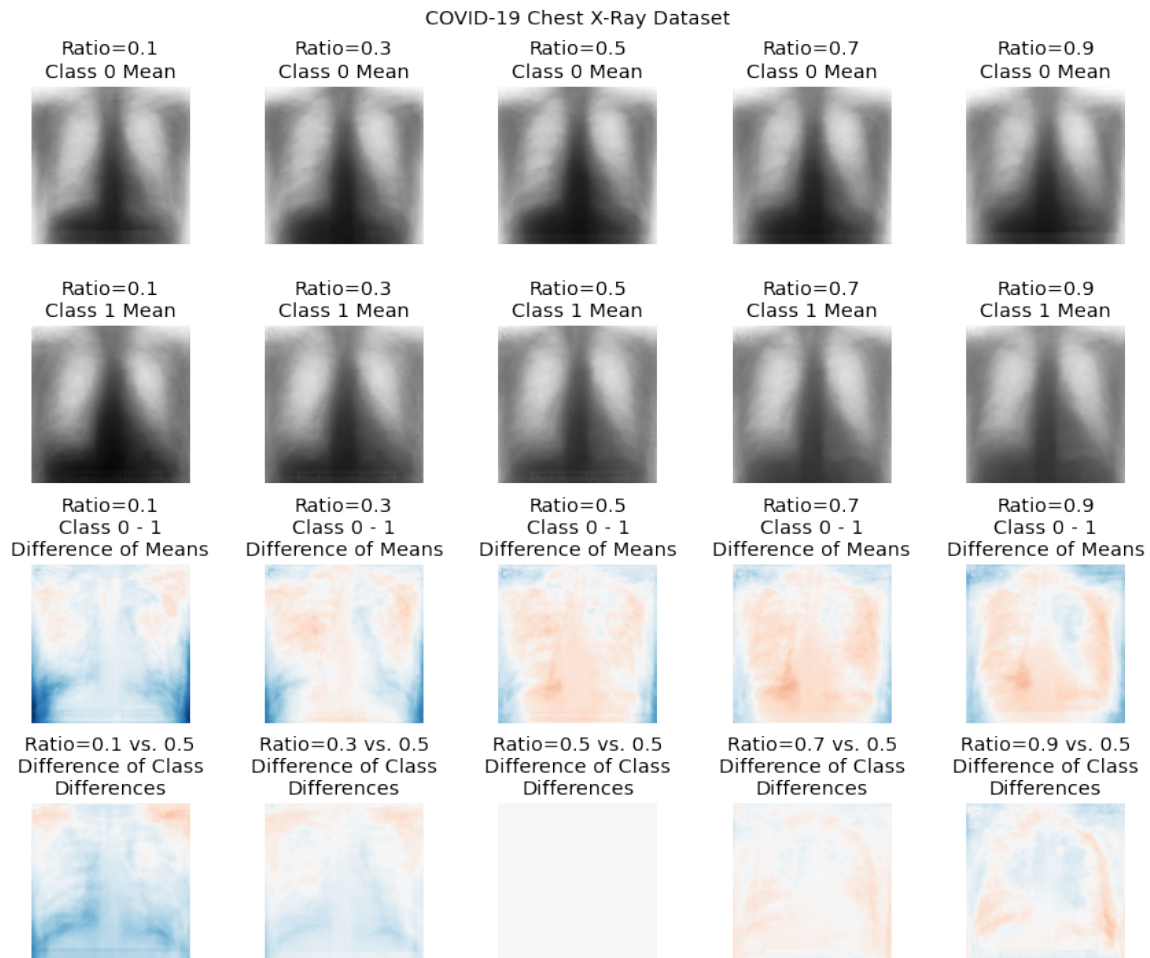


Figure 4: An example of the mean class difference drawn from the COVID-19 dataset at different covariate ratios. Here, the first COVID-19 dataset consisted of only AP images, whereas the second dataset consisted of only PA images. The third row shows, for each ratio, the difference in the class means, demonstrating the effect of sampling images from the two views on the perceived class difference. The fourth row shows the difference between each ratio’s difference image, and the difference image with a ratio of 0.5 (balanced sampling from all views).

## Appendix D. Transfer Learning Example

This is an example of fine-tuning a pre-trained model on a dataset which is in the TorchXRayVision format. This code is available online<sup>2</sup>.

```
# Use XRV transforms to crop and resize the images
transforms = torchvision.transforms.Compose([xrv.datasets.XRayCenterCrop(),
                                           xrv.datasets.XRayResizer(224)])

# Load Google dataset and PyTorch dataloader
dataset = xrv.datasets.NIH_Google_Dataset(imgpath=dataset_dir,
                                          transform=transforms)
dataloader = torch.utils.data.DataLoader(dataset, batch_size=8)

# Load pre-trained model and erase classifier
model = xrv.models.DenseNet(weights="densenet121-res224-all")
model.op_threshs = None # prevent pre-trained model calibration
model.classifier = torch.nn.Linear(1024,1) # reinitialize classifier

optimizer = torch.optim.Adam(model.classifier.parameters()) # only train classifier
criterion = torch.nn.BCEWithLogitsLoss()

# training loop
for batch in dataloader:
    outputs = model(batch["img"])
    targets = batch["lab"][:, dataset.pathologies.index("Lung Opacity"), None]
    loss = criterion(outputs, targets)
    loss.backward()
    optimizer.step()
```

---

2. [https://github.com/mlmed/torchxrayvision/blob/master/scripts/transfer\\_learning.ipynb](https://github.com/mlmed/torchxrayvision/blob/master/scripts/transfer_learning.ipynb)